

Multiband effects on the Fulde-Ferrell-Larkin-Ovchinnikov state in superconducting metallic nanofilms.

P. Wójcik¹, M. Zegrodnik²

¹AGH University of Science and Technology, Faculty of Physics and Applied
Computer Science, al. Mickiewicza 30, Kraków, Poland

²AGH University of Science and Technology, Academic Centre for Materials and
Nanotechnology, Al. Mickiewicza 30, 30-059 Kraków, Poland

E-mail: pawel.wojcik@fis.agh.edu.pl, michal.zegrodnik@gmail.com

PACS numbers: 74.78.-w

Submitted to: *Superconductor Science and Technology*

Abstract. In superconducting nanofilms the energy quantization induced by the confinement in the direction perpendicular to the film leads to a multiband character of the system which results in the thickness-dependent oscillations of the in-plane critical field (shape resonances). In this paper, we study the Fulde-Ferrel-Larkin-Ovchinnikov (FFLO) phase in nanofilms and examine its interplay with the shape resonances as well as the influence of the multiband effects on its stability. We demonstrate that the range of the magnetic field for which the FFLO state is stable oscillates as a function of the film thickness with the phase shift equal to one half of the period corresponding to the critical magnetic field oscillations. Moreover, the multiband effects lead to a division of the FFLO phase stability region into subregions number of which depends on the number of bands participating in the formation of the paired state.

1. Introduction

The superconducting Fulde-Ferrel-Larkin-Ovchinnikov (FFLO) phase is characterized by the nonzero total momentum of the Cooper pairs. According to the original idea, proposed by Fulde and Ferrel [1] as well as independently by Larkin and Ovchinnikov [2], the nonzero momentum pairing appears in the presence of external magnetic field as a consequence of the Fermi wave vector mismatch between particles from two spin subbands with opposite momenta. Such unconventional paired state can survive in magnetic fields higher than the second critical field H_{c2} . In spite of many theoretical studies regarding the FFLO state [3, 4, 5, 6], the experimental signs of the nonzero momentum pairing have been reported only recently in the heavy fermion systems [7, 8, 9, 10] and the two dimensional organic superconductors [11, 12, 13, 14]. The difficulties in experimental observation of the FFLO state are caused by the stringent conditions for its appearance. First of all, the high value of the Maki parameter is essential, which means that the Pauli paramagnetic effect has to be strong relative to the orbital pair-breaking mechanism being detrimental to the FFLO state [15]. Moreover, the system has to be ultra clean as the FFLO phase is easily destroyed by the impurities [16, 17].

The ultra thin metallic nanofilms which can be fabricated due to the huge development of nanotechnology [18, 19, 20, 21, 22, 23, 24] may satisfy the conditions for the FFLO phase appearance. In the nanofilms subjected to the parallel magnetic field, the confinement in the direction perpendicular to the film reduces the orbital effect leading to a high value of the Maki parameter. However, if the size of the system becomes comparable to the electron's wave length, the Fermi sphere splits into a set of discrete two-dimensional subbands leading to the multiband character of the system. The multiband effects caused by the confinement lead to the thickness-dependent oscillations of the superconducting properties (shape resonances). So far, the thickness-dependent oscillations of the energy gap [25, 26], critical temperature [18, 19, 20, 21, 27, 28], and critical magnetic field [29, 30, 31, 32, 33] have been experimentally observed, as well as theoretically studied. In spite of the multiband behavior of a variety of superconductors, such as MgB_2 or the iron-based superconductors [34, 35], the FFLO

phase with the inclusion of the multiband effect has been the subject of only a few papers. Theoretical investigations regarding the FFLO phase appearance in a multiband model corresponding to the iron-pnictides have been presented in Refs. [36, 37]. Very recently we have suggested that the non-zero momentum paired phase can appear in the absence of the external magnetic field in $\text{LaFeAsO}_{1-x}\text{F}_x$ with a predominant interband pairing [38]. Furthermore, the multiband effects on the FFLO phase in a Pauli-limiting two-band superconductor have been theoretically studied in Refs. [39, 40]. In these studies [39, 40] it has been found that a competing effect can arise from the coupling in two bands each of which has their own favorable momentum of the Cooper pairs. This gives rise to a rich FFLO phase diagram with the subregions corresponding to different Cooper pair momenta.

In the present paper we consider free-standing $\text{Pb}(111)$ metallic nanofilms in the presence of the in-plane magnetic field and investigate the formation of the FFLO phase as well as its interplay with the multiband character of the system. In our considerations the number of subbands is determined by the nanofilm thickness. We have shown that the shape resonance conditions are detrimental to the FFLO phase formation. As a consequence, the magnetic field for which the FFLO state is stable oscillates as a function of the film thickness with the phase shift equal to one half of the period corresponding to the critical magnetic field oscillations. Moreover, the multiband effects lead to a division of the FFLO phase stability region into subregions number of which depends on the number of bands participating in the formation of the paired state.

The paper is organized as follows: in Sec. 2 we introduce the basic concepts of the theoretical scheme based on the BCS theory. In Sec. 3 we present the results while the summary is included in Sec. 4.

2. Theoretical method

We start with the BCS Hamiltonian in the presence of external in-plane magnetic field $\mathbf{H}_{||} = (H_{||}, 0, 0)$

$$\begin{aligned} \hat{\mathcal{H}} = & \sum_{\sigma} \int d^3r \hat{\Psi}^{\dagger}(\mathbf{r}, \sigma) \hat{H}_e^{\sigma} \hat{\Psi}(\mathbf{r}, \sigma) \\ & + \int d^3r \left[\Delta(\mathbf{r}) \hat{\Psi}^{\dagger}(\mathbf{r}, \uparrow) \hat{\Psi}^{\dagger}(\mathbf{r}, \downarrow) + H.c. \right] + \int d^3r \frac{|\Delta(\mathbf{r})|^2}{g}, \end{aligned} \quad (1)$$

where σ corresponds to the spin state (\uparrow, \downarrow), g is the phonon-mediated electron-electron coupling constant, while $\Delta(\mathbf{r})$ is the superconducting gap parameter in real space defined as

$$\Delta(\mathbf{r}) = -g \left\langle \hat{\Psi}(\mathbf{r}, \downarrow) \hat{\Psi}(\mathbf{r}, \uparrow) \right\rangle. \quad (2)$$

The single-electron Hamiltonian \hat{H}_e^{σ} is given by

$$\hat{H}_e^{\sigma} = \frac{1}{2m} \left(-i\hbar\nabla + \frac{e}{c}\mathbf{A} \right)^2 + s\mu_B H_{||} - \mu_F, \quad (3)$$

where $s = +1(-1)$ for $\sigma = \uparrow(\downarrow)$, m is the effective electron mass, μ_F is the chemical potential, and we have chosen the gauge for the vector potential as $\mathbf{A} = (0, -H_{\parallel}z, 0)$. Due to the confinement of electrons in the direction perpendicular to the film (z axis) the quantization of the energy appears. Thus, the field operators in Eq.(1) have the form

$$\hat{\Psi}(\mathbf{r}, \sigma) = \sum_{\mathbf{k}n} \phi_{\mathbf{k}n}(\mathbf{r}) \hat{c}_{\mathbf{k}n\sigma}, \quad \hat{\Psi}^\dagger(\mathbf{r}, \sigma) = \sum_{\mathbf{k}n} \phi_{\mathbf{k}n}^*(\mathbf{r}) \hat{c}_{\mathbf{k}n\sigma}^\dagger, \quad (4)$$

where $\hat{c}_{\mathbf{k}n\sigma}(\hat{c}_{\mathbf{k}n\sigma}^\dagger)$ is the annihilation (creation) operator for an electron with spin σ in a state characterized by the quantum numbers (\mathbf{k}, n) . The single-electron eigenfunctions $\phi_{\mathbf{k}n}(\mathbf{r})$ of the Hamiltonian \hat{H}_e^σ are given below

$$\phi_{\mathbf{k}n}(\mathbf{r}) = \frac{1}{2\pi} e^{ik_x x} e^{ik_y y} \varphi_{k_y n}(z), \quad (5)$$

where $\mathbf{k} = (k_x, k_y)$ is the electron wave vector, while n labels the discrete quantum states. We determine $\varphi_{k_y n}(z)$ by diagonalization of the Hamiltonian (3) in the basis of the quantum well states

$$\varphi_{k_y n}(z) = \sqrt{\frac{2}{d}} \sum_l c_{k_y l} \sin \left[\frac{\pi(l+1)z}{d} \right], \quad (6)$$

where d is the nanofilm thickness. We use the hard-wall potential as the boundary condition for the wave function in the z -direction.

In the FFLO phase, induced by the magnetic field, the Cooper pairs gain the nonzero total momentum \mathbf{q} which results from the pairing of electrons from spin-split subbands $[(\mathbf{k}, n), (-\mathbf{k} + \mathbf{q}n)]$. For such pairing, the substitution of the expression for the gap parameter 2) and the field operators (4) into Eq. (1) gives the following form of the Hamiltonian

$$\begin{aligned} \hat{\mathcal{H}} = & \sum_{\mathbf{k}n} (\hat{c}_{\mathbf{k}n\uparrow}^\dagger \hat{c}_{-\mathbf{k}+\mathbf{q}n\downarrow}) \begin{pmatrix} \xi_{\mathbf{k}n} & \Delta_{\mathbf{q}n} \\ \Delta_{\mathbf{q}n} & -\xi_{-\mathbf{k}+\mathbf{q}n} \end{pmatrix} \begin{pmatrix} \hat{c}_{\mathbf{k}n\uparrow} \\ \hat{c}_{-\mathbf{k}+\mathbf{q}n\downarrow}^\dagger \end{pmatrix} \\ & + \sum_{\mathbf{k}n} \xi_{-\mathbf{k}+\mathbf{q}n} + \sum_n \frac{|\Delta_{\mathbf{q}n}|^2}{g}, \end{aligned} \quad (7)$$

where \mathbf{q} is the total momentum of the Cooper pairs in the (x, y) plane. Analogously as in the paper by Fulde and Ferrell [1] we have assumed that all the Cooper pairs have the same momentum \mathbf{q} . The direction of \mathbf{q} is arbitrary for the case of s-wave pairing symmetry with parabolic dispersion relation. For simplicity we take on $\mathbf{q} = (q, 0)$. The energy gap in reciprocal space is defined as

$$\Delta_{\mathbf{q}n'} = \frac{g}{4\pi^2} \sum_{\mathbf{k}n} C_{\mathbf{k}n'n} \langle \hat{c}_{-\mathbf{k}+\mathbf{q}n\downarrow} \hat{c}_{\mathbf{k}n\uparrow} \rangle, \quad (8)$$

where

$$C_{\mathbf{k}n'n} = \int dz \varphi_{k_y n'}(z) \varphi_{-k_y n'}(z) \varphi_{k_y n}(z) \varphi_{-k_y n}(z). \quad (9)$$

The Hamiltonian (7) can be reduced to the diagonal form by the Bogoliubov-de Gennes transformation $\hat{c}_{\mathbf{k}n\sigma} = u_{\mathbf{k}n\sigma}\gamma_{\mathbf{k}n} + sv_{\mathbf{k}n\sigma}^*\gamma_{\mathbf{k}n}^\dagger$ [41]. As a result, one obtains the following form of the quasiparticle energies

$$E_{\mathbf{k}\mathbf{q}n}^\pm = \frac{1}{2} (\xi_{\mathbf{k}n} - \xi_{-\mathbf{k}+\mathbf{q}n} \pm \sqrt{\alpha_{\mathbf{k}\mathbf{q}n}}) + \mu_B H, \quad (10)$$

with

$$\alpha_{\mathbf{k}\mathbf{q}n} = (\xi_{\mathbf{k}n} + \xi_{-\mathbf{k}+\mathbf{q}n})^2 + 4\Delta_{\mathbf{q}n}^2. \quad (11)$$

The self-consistent equation for the superconducting gaps (for n bands we have n gap parameters) has the form

$$\Delta_{\mathbf{q}n'} = \frac{g}{4\pi^2} \sum_{\mathbf{k}n} C_{\mathbf{k}n'n} \frac{\Delta_{\mathbf{q}n}}{\sqrt{\alpha_{\mathbf{k}\mathbf{q}n}}} [1 - f(E_{\mathbf{k}\mathbf{q}n}^+) - f(E_{\mathbf{k}\mathbf{q}n}^-)], \quad (12)$$

where $f(E)$ is the Fermi-Dirac distribution. The summation in Eq. (12) is carried out only over the single-electron states with energy $\xi_{\mathbf{k}n}$ inside the Debye window $|\xi_{\mathbf{k}n}| < \hbar\omega_D$, where ω_D is the Debye frequency. Since the chemical potential μ for nanofilms can strongly deviates from its bulk value μ_{bulk} for each nanofilm thickness we calculate μ using the expression

$$n_e = \frac{1}{d} \sum_{\mathbf{k}n} \int_0^d dz \left\{ |u_{\mathbf{k}\mathbf{q}n} \varphi_{k_y n}(z)|^2 f(E_{\mathbf{k}\mathbf{q}n}) + |v_{\mathbf{k}\mathbf{q}n} \varphi_{k_y n}(z)|^2 [1 - f(E_{\mathbf{k}\mathbf{q}n})] \right\}, \quad (13)$$

where n_e is the electron density corresponding to the bulk value (it refers to the chemical potential μ_{bulk}) and $u_{\mathbf{k}\mathbf{q}n}$, $v_{\mathbf{k}\mathbf{q}n}$ are the Bogolubov coherence factors.

After calculating the superconducting gaps in the reciprocal space $\Delta_{\mathbf{q}n}$ one can determine the spatial dependence of the order parameter by using the following formula

$$\Delta_{\mathbf{q}}(\mathbf{r}) = e^{i\mathbf{q}\cdot\mathbf{r}} \Delta_{\mathbf{q}}(z), \quad (14)$$

where

$$\Delta_{\mathbf{q}}(z) = \frac{g}{4\pi^2} \sum_{\mathbf{k}n} \varphi_{k_y n}(z) \varphi_{-k_y n}(z) \frac{\Delta_{\mathbf{q}n}}{\sqrt{\alpha_{\mathbf{k}\mathbf{q}n}}} [1 - f(E_{\mathbf{k}\mathbf{q}n}^+) - f(E_{\mathbf{k}\mathbf{q}n}^-)]. \quad (15)$$

As one can see the spatial dependence of the superconducting gap in the (x, y) plane is due to the nonzero center of mass momentum of the Cooper pairs while the z -dependence comes from the confinement of the electrons within the nanofilm. In the further analysis we often use the spatially averaged energy gap defined as

$$\bar{\Delta}_{\mathbf{q}} = \frac{1}{d} \int_0^d \Delta_{\mathbf{q}}(z) dz. \quad (16)$$

To obtain the results presented in the next section, the set of self-consistent equations (12), (13) is calculated numerically and the Cooper pair total momentum \mathbf{q} is determined by minimizing the free energy of the system [42].

3. Results

In the present paper we consider the FFLO phase induced by the in-plane magnetic field in free-standing Pb(111) nanofilms. The first-principle calculations of the electronic structure for Pb nanofilms [43, 44, 45] demonstrated that the quantum size effect for Pb(111) can be well described by the quantum well states centered at the L-point of a two-dimensional Brillouin zone [43]. Moreover, the energy dispersion calculated for Pb(111) nanofilms is nearly parabolic [43]. Based on these results, in our calculations we use the parabolic band approximation treating the bulk Fermi level μ_{bulk} and the electron mass m as the fitting parameters. Their values are determined based on the results from the first principle calculations presented in Refs. [43]. In our study we use the following values of the parameters: $gN_{bulk}(0) = 0.39$ where $N_{bulk}(0) = mk_F/(2\pi^2\hbar^2)$ is the bulk density of the single-electron states at the Fermi level, $\hbar\omega_D = 8.27$ meV, the bulk critical temperature $T_{bulk} = 7.2$ K corresponding to the energy gap $\Delta_{bulk} = 1.1$ meV and $\mu_{bulk} = 3.8$ eV which corresponds to the electron density $n_e = 4.2 \times 10^{21} \text{ cm}^{-3}$. Since the calculations for the FFLO phase in nanofilms are time-consuming we restrict our analysis to the temperature $T = 0$ K.

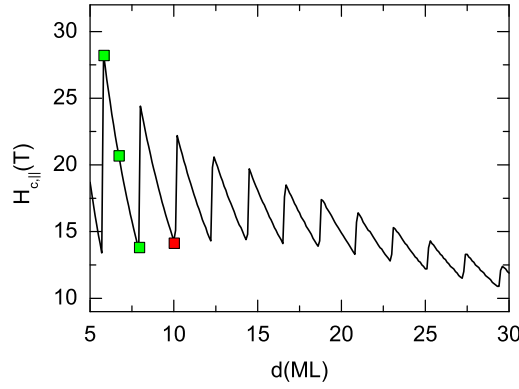


Figure 1. (Color online) In-plane critical magnetic field $H_{c,||}$ as a function of the nanofilm thickness d calculated without the inclusion of the FFLO phase for $\mathbf{q} = 0$ and $T = 0$ K. Squares denote the film thicknesses chosen for the analysis of the FFLO phase stability.

Figure 1 displays the in-plane critical field $H_{c,||}$ as a function of the nanofilm thickness d calculated assuming $\mathbf{q} = 0$ (no FFLO phase). The 'tooth-like' oscillations presented in Fig. 1 are well known [28, 33] and can be explained on the basis of the electron energy quantization. If the confinement of the electron motion in the direction perpendicular to the film becomes comparable to the electrons wave length, the Fermi sphere splits into a set of discrete two-dimensional parabolic subbands. The energies of these subbands decrease with increasing nanofilm thickness. Each time a subband passes through the Fermi level the density of states in the energy window $[\mu - \hbar\omega_D, \mu + \hbar\omega_D]$, in which the phonon-mediated pairing occurs, abruptly increases leading to the increase of

the critical magnetic field. This phenomenon is called 'shape resonance'. In the further analysis we use the term resonant and non-resonant thickness to define the thickness for which the resonance conditions are satisfied or not satisfied, respectively. Therefore, the thickness-dependent oscillations of $H_{c,\parallel}$ presented in Fig. 1 are caused by the subsequent subbands passing through the Fermi level while the nanofilm thickness is increased. A detailed analysis of this effect can be found in our recent paper [32].

First, we discuss the ultrathin nanofilm with the thickness $d = 3$ ML (not marked in Fig. 1). For such a thin film the in-plane magnetic field acts only on the spins of the conduction electrons and all orbital effects can be neglected. The corresponding quasiparticle dispersion relation and the z -dependence of the superconducting gap are shown in Fig. 2. For the chosen thickness only the lowest band participates in the paired phase, therefore, the multiband effects on the superconducting state do not appear. In

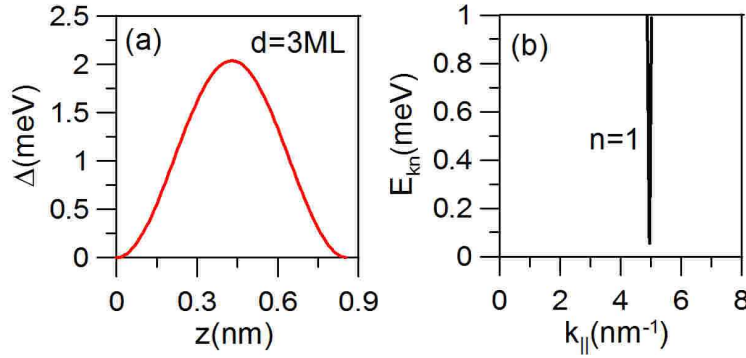


Figure 2. (Color online) (a) Spatially dependent superconducting gap $\Delta(z)$ and (b) quasi-particle band which participates in the formation of the superconducting state. Results for the nanofilm thickness $d = 3$ ML and $H_{\parallel} = 0$.

Fig. 3(a) we plot the spatially averaged energy gap $\bar{\Delta}$ as a function of the magnetic field H_{\parallel} . The values of the Cooper pair momentum q which correspond to the stability of the FFLO phase are shown in Fig. 3(b) and have been determined by minimizing the free energy F of the system. The dependences $F(q)$ for the superconducting and normal phases calculated for $H_{\parallel} = 18.5$ T are displayed in Fig. 3(c). The free energy minimum, marked by arrow, corresponds to stable FFLO state. Fig. 3(a) shows that the transition from the BCS to the FFLO phase has a discontinuous nature whereas in the FFLO region, the spatially averaged energy gap decreases almost linearly with increasing magnetic field. The presented behavior agrees with the one reported for single-band s -wave superconductors [7].

As explained above, in nanofilms, the number of bands participating in the superconducting state depends on the thickness, d . If we increase the nanofilm thickness, the subsequent subbands begin to participate in the superconducting phase giving rise to the shape resonances presented in Fig. 1. In order to analyze the interplay between the shape resonances and the stability of the FFLO phase, in Fig. 4 (left panels) we present the spatially averaged energy gap $\bar{\Delta}$ as a function of the magnetic field H_{\parallel} for different

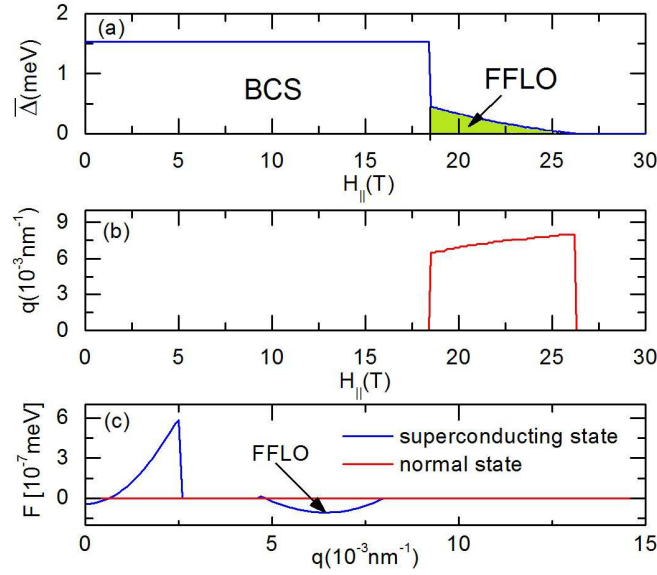


Figure 3. (Color online) (a) Spatially averaged energy gap $\bar{\Delta}$ as a function of the magnetic field $H_{||}$ (the FFLO phase stability is marked by the green region). (b) Total momentum of the Cooper pairs q , which corresponds to the stable FFLO state, as a function of the magnetic field $H_{||}$. (c) Free energy F of the superconducting and normal states as functions of the Cooper pairs total momentum q . Results for the nanofilm thickness $d = 3$ ML.

nanofilm thicknesses: (a) $d = 5.8$ ML which corresponds to the shape resonance, (b) $d = 6.75$ ML in the middle between two adjacent resonances and (c) $d = 7.9$ ML for which the resonance conditions are not satisfied. The nanofilm thicknesses chosen for the analysis are marked by the green squares in Fig. 1. Right panels in Fig. 4 present the total momentum of the Cooper pairs which correspond to the stability of the FFLO phase. In comparison with the results for the thickness $d = 3$ ML (see Fig. 3) the stability range of the FFLO phase is narrowed down due to the multiband and orbital effects. From the presented results one can see that the range of the FFLO phase stability is minimal for the thickness corresponding to the shape resonance $d = 5.8$ ML [see Fig. 3(a)], then it gradually increases to its maximal value for $d = 7.9$ ML, for which the shape resonance conditions are not satisfied. The same behavior is observed for other resonances depicted in Fig. 1. Based on these results one can distinguish two characteristic features: (i) the shape resonance conditions are detrimental to the FFLO state formation, and (ii) the range of the magnetic field for which the FFLO phase is stable oscillates as a function of the film thickness with the phase shift equal to one half of the period corresponding to the critical field oscillations.

The presented behavior can be explained on the basis of the multiband nature of the considered system. For a given nanofilm thickness a particular number of subbands participate in the superconducting state. In the presence of the magnetic field the wave vector mismatch (induced by the Zeeman spin splitting), which corresponds to different subbands, may vary significantly. As a consequence, each subband has its

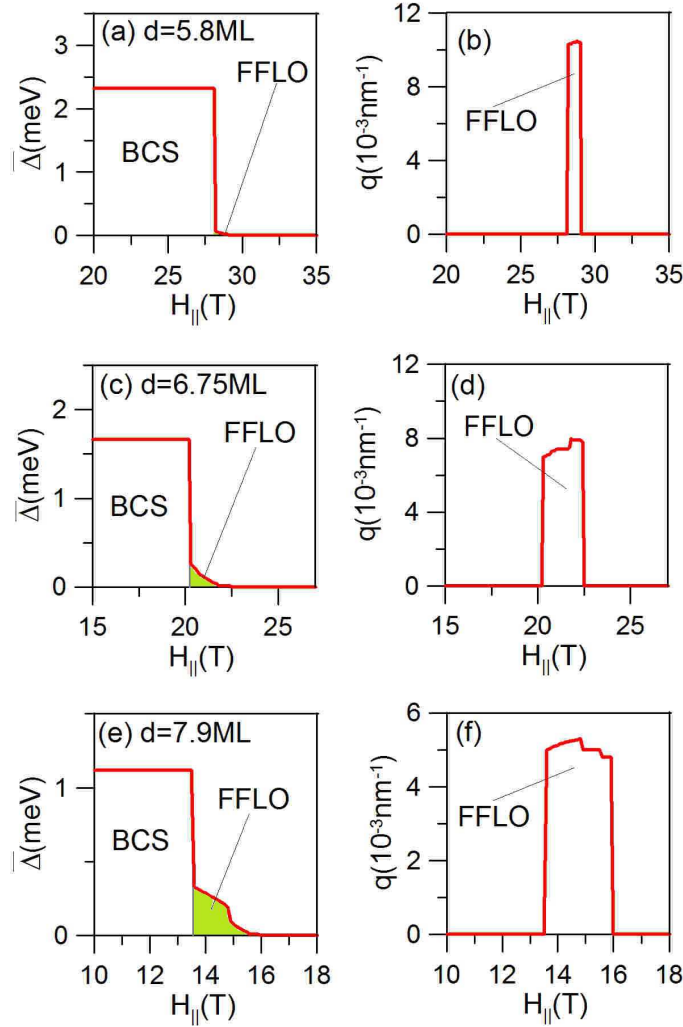


Figure 4. (Color online) (a) Spatially averaged energy gap $\bar{\Delta}$ (left panels) and total momentum of Cooper pairs (right panels) as functions of the magnetic field $H_{||}$ for the nanofilm thickness (a,b) $d = 5.8$ ML, (c,d) $d = 6.75$ ML and (e,f) $d = 7.9$ ML. The chosen nanofilm thicknesses are marked by the green squares in Fig. 1.

own favorable value of the Cooper pair total momentum q_n . However, the situation in which there is a number of independent modulation vectors q_n simultaneously, each corresponding to a different subband, cannot be realized in the system because all the subband gap parameters Δ_{q_n} are coupled (c.f. Eq. 12). Since there can be only one value of the Cooper pair total momentum in the system, a competition between the subbands appears. For the resonant thicknesses there is one leading quasi-particle branch n' (with the energy gap Δ'_n) which is responsible for the enhancement of the paired phase [26]. Its dominant influence on the formation of the superconducting state results from the high density of states at the Fermi level which appears each time when the bottom of a subband is close to the Fermi level. However, the closer to the Fermi level the bottom of a subband is, the greater is the wave vector mismatch which corresponds to this subband in the presence of magnetic field. Therefore, for the leading quasi-particle

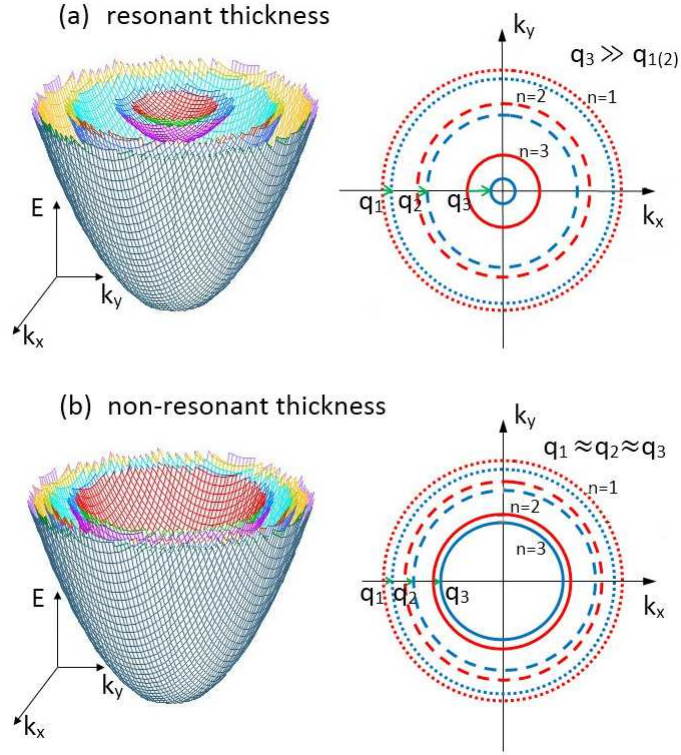


Figure 5. (Color online) Schematic illustration of the single electron parabolic subbands (left panels) and their intersections at the Fermi energy (right panels) for (a) resonant thickness and (b) non-resonant thickness. The red and blue color in the right panel corresponds to the spin-up and spin-down subbands, respectively. The Fermi wave vector mismatch between spin-split subbands, induced by the magnetic field, can be compensated by the non-zero total momentum of the Cooper pairs. The Cooper pair momenta q_n corresponding to all subbands are marked by green arrows in the right panels.

branch the favored Cooper pair momentum $q_{n'}$ is significantly greater than the ones which correspond to the remaining bands, as schematically presented in Fig. 5(a). Due to this fact it is not possible to adjust a single Cooper pair total momentum in order to compensate all the wave vector mismatches, what leads to the suppression of the FFLO phase. On the other hand, for the film thicknesses for which the resonance conditions are not fulfilled (non-resonant thickness), the contribution to the superconducting BCS phase coming from all the subbands is comparable. Since the energies corresponding to the bottoms of all the subbands are far below the Fermi level the total momenta of the Cooper pairs q_n which compensate the wave vector mismatches for all the subbands differ only slightly as presented in Fig. 5(b). In such situation it is possible to adjust the q vector to compensate each Fermi wave vector mismatch to a large extent. In this case, the FFLO phase stability range reaches its maximal value.

In Fig. 6 we present the quasi-particle branches and the spatially dependent energy gap for two thicknesses corresponding to Fig. 4, $d = 5.8$ ML (resonant thickness) and

$d = 7.9$ ML (non-resonant thickness) calculated for $H_{||} = 0$ (due to the symmetry $k_x - k_y$ for $H_{||} = 0$ we can define $k_{||}^2 = k_x^2 + k_y^2$). As we can see the three lowest bands

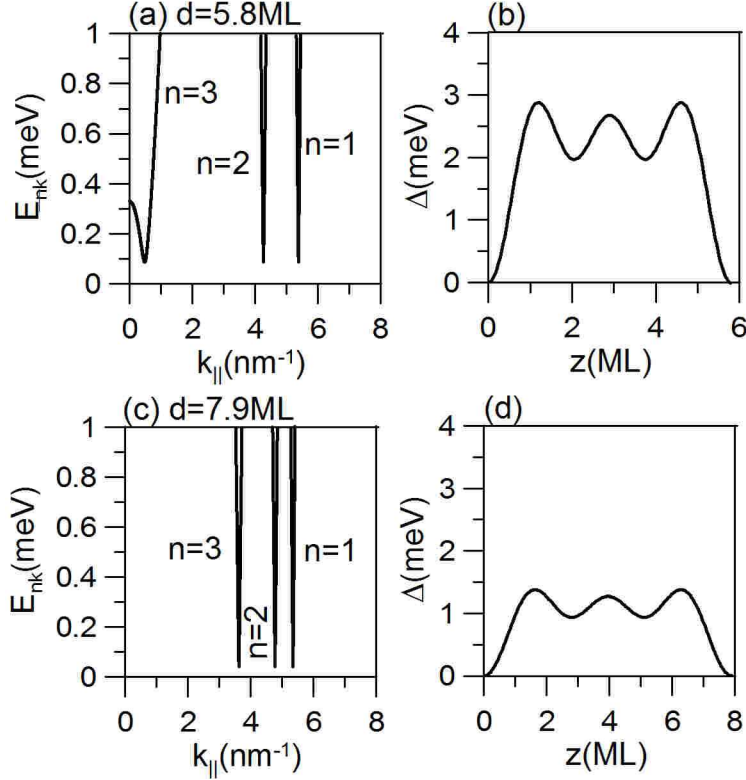


Figure 6. (Color online) Quasi-particle subbands E_{kn} and spatially dependent energy gap for (a) the resonant thickness $d = 5.8$ ML and (b) the non-resonant thickness $d = 7.9$ ML.

contribute to the superconducting state for both thicknesses. The shape resonance for $d = 5.8$ ML results from the pairing in the subband $n = 3$, as the bottom of this subband has just passed through the Fermi level. As aforementioned, this dominant resonant subband leads to the enhancement of the energy gap [compare Fig.6(b) and (d)] and is detrimental to the FFLO state formation. On the other hand, for the non-resonant thickness $d = 7.9$ ML the three subbands are far below the Fermi energy. Since they have comparable total momentum of the Cooper pairs the adjustment of a single q vector for all the bands is possible giving raise to the FFLO state stability region.

As it has already been mentioned for the case of multiband superconductors the competing effect leads to a complex structure of the FFLO state stability region, which is divided into N subregions, with N being the number of superconducting subbands. Such behavior is presented in Fig. 7 which shows the data from Fig.4(e) but limited to the FFLO phase stability region. In Fig. 7 one can distinguish between three FFLO phases, labeled by FFLO- n ($n=1,2,3$). For a given FFLO- n phase the total momentum q of the Cooper pairs is mainly determined by the Fermi wave vector mismatch in the n -th band. Similar behavior is observed for the rest of non-resonant thicknesses. In

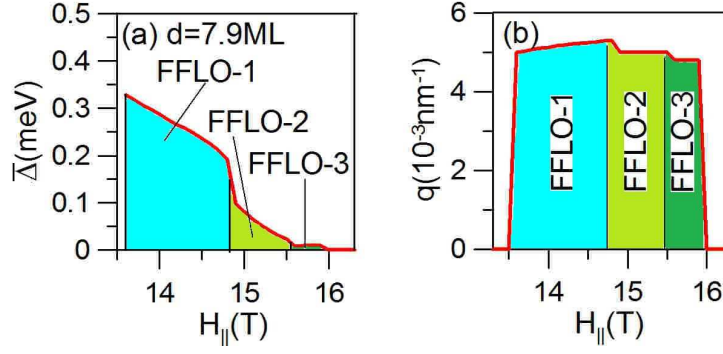


Figure 7. (Color online) (a) Spatially averaged energy gap $\bar{\Delta}$ and (b) total momentum of the Cooper pairs q corresponding to stable FFLO state as a function of the magnetic field $H_{||}$. Results presented for the same data as in Fig. 4(e) but limited to the FFLO phase stability region. Different FFLO subphases are marked by different colors and labeled by FFLO- n ($n = 1, 2, 3$).

Fig. 8 we present the FFLO stability region for $d = 10$ ML which corresponds to the non-resonant thickness in which four subbands participate in the superconducting state (denoted by the red square in Fig. 1). By analogy, the FFLO stability region is now divided into four subregions.

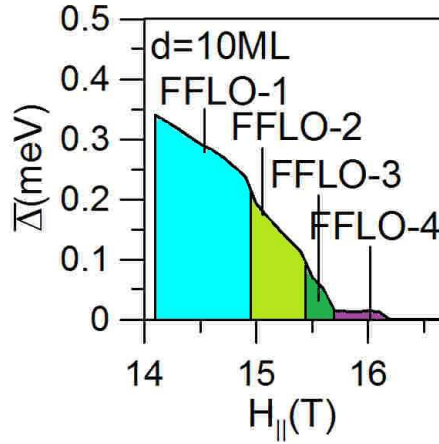


Figure 8. (Color online) (a) Spatially averaged energy gap $\bar{\Delta}$ as a function of the magnetic field $H_{||}$ for the thickness $d = 10$ ML (marked by red square in Fig. 1). Results limited to the FFLO phase stability region. Different FFLO subphases are marked by different colors and labeled by FFLO- n ($n = 1, 2, 3, 4$).

Further increase of the thickness makes the orbital effect more relevant what is detrimental to the FFLO state formation. Due to the orbital effect the range of the magnetic field in which the FFLO state exists gradually decreases with increasing film thickness and for d greater than 15 ML this phase completely disappears.

4. Summary

The multiband effects on the FFLO state induced by the in-plane magnetic field in Pb(111) nanofilms has been investigated in the framework of the BCS theory. We have studied the interplay between the FFLO phase and the shape resonances, as well as the influence of the multiband and orbital effects on its stability. We have found that for the resonant thicknesses the FFLO phase stability region is suppressed due the difference between the Fermi wave vector mismatch corresponding the resonant subband and the one corresponding to the remaining subbands. As a consequence, the range of the magnetic field for which the FFLO phase is stable oscillates as a function of the film thickness with the phase shift equal to one half of the period corresponding to the critical field oscillations. Moreover, we have found that the FFLO stability region is divided into N subregions where N is the number of subbands which contribute to the superconducting state.

It is worth mentioning that so far there have been no reports on the FFLO phase stability in metallic nanofilms. This fact is mainly due to the quality of the films most of which are in the dirty limit while the non-zero momentum paired phase is easily destroyed by the nonmagnetic impurities [16, 17]. Other experimental difficulties such as surface roughness or the magnetic field direction, which has to be applied precisely parallel to the plane, are also detrimental to the FFLO phase formation. Nevertheless, one can hope that the technological progress will allow for the fabrication of very clean nanofilms in the future and investigate experimentally some of the effects studied theoretically in this paper.

Acknowledgments

This work was financed from the budget for Polish Science in the years 2013-2015. Project number: IP2012 048572. M. Z. acknowledges the financial support from the Foundation for Polish Science (FNP) within project TEAM.

References

- [1] P Fulde and A Ferrell. *Phys. Rev.*, 135:A550, 1964.
- [2] A I Larkin and Yu N Ovchinnikov. *Zh. Eksp. Teor. Fiz.*, 47:1136, 1964.
- [3] H Shimahara. *Phys. Rev. B*, 50:12760, 1994.
- [4] R Casalbuoni and G Narduli. *Rev. Mod. Phys.*, 76:263, 2004.
- [5] A Ptok, M M Maška, and M Mierzejewski. *J. Phys. Condens. Matter*, 21:295601, 2009.
- [6] M M Maška, M Mierzejewski, J Kaczmarczyk, and J Spalek. *Phys. Rev. B*, 82:054509, 2010.
- [7] Y Matsuda and H Shimahara. *J. Phys. Soc. Jpn.*, 76:051005, 2007.
- [8] A Bianchi, R Movshovich, C Capan, P G Pagluso, and J L Sarrao. *Phys. Rev. Lett.*, 91:187004, 2003.
- [9] K Kumagai, M Saitoh, T Oyaizu, Y Furukawa, S Takashima, M Nohara, H Takagi, and Y Matsuda. *Phys. Rev. Lett.*, 97:227002, 2006.
- [10] V F Correa, T P Murphy, C Martin, K M Purcell, E C Palm, G M Schmiedenshoff, J C Cooley, and W Tozer. *Phys. Rev. Lett.*, 98:087001, 2007.

- [11] R Beyer and J Wosnitzer. *Low Temp. Phys.*, 39:225, 2013.
- [12] J Singleton, J A Symington, M S Nam, A Ardavan, and M Kurmoo. *J. Phys. Condens. Matter*, 12:L641, 2000.
- [13] M A Tanatar, T Ishiguro, H Tanaka, and H Kobayashi. *Phys. Rev. B*, 66:124503, 2002.
- [14] Y Shinagawa, Ja nd Kurosaki, F Zhang, C Parker, S E Brown, D Jerome, J B Christensen, and K Bechgaard. *Phys. Rev. Lett.*, 98:147002, 2002.
- [15] L W Gruenberg and L Gunther. *Phys. Rev. Lett.*, 16:996, 1966.
- [16] L G Aslamazov. *Sov. Phys. JETP*, 28:773, 1969.
- [17] S Takada. *Prog. Theor. Phys.*, 43:27, 1970.
- [18] M M Özer, J R Thompson, and H H Weitering. *Nat. Phys.*, 2:173, 2006.
- [19] M M Özer, J R Thompson, and H H Weitering. *Phys. Rev. B*, 74:235427, 2006.
- [20] Y Guo, Y F Zhang, X Y Bao, T Z Han, Z Tang, L X Zhang, W G Zhu, E G Wang, Q Niu, Z Q Qiu, J F Jia, Z X Zhao, and Q K Xue. *Science*, 306:1915, 2004.
- [21] D Eom, S Qin, M Y Chou, and C K Shih. *Phys. Rev. Lett.*, 96:027005, 2006.
- [22] T Zhang, P Cheng, W J Li, Y J Sun, X G Wang G, Zhu, K He, L L Wang, X C Ma, X Chen, Y Y Wang, Y Liu, Lin H Q, J F Jia, and Q K Xue. *Nat. Phys.*, 6:104, 2010.
- [23] T Uchihashi, P Mishra, M Aono, and T Nakayama. *Phys. Rev. Lett.*, 107:207001, 2011.
- [24] S Qin, J Kim, Q Niu, and C K Shih. *Science*, 324:1314, 2009.
- [25] N A Court, J Ferguson, A, and R G Clark. *Supercond. Sci. Technol.*, 21:015013, 2007.
- [26] A A Shanenko, M D Croitoru, and F M Peeters. *Phys. Rev. B*, 75:014519, 2007.
- [27] M M Özer, Y Jia, Z Zhang, J R Thompson, and H H Weitering. *Science*, 316:1594, 2007.
- [28] P Wójcik and M Zegrodnik. *phys. stat. sol. (b)*, 251:1069, 2014.
- [29] X Y Bao, Y F Zhang, Y Wang, J F Jia, Q K Xue, X C Xie, and Z X Zhao. *Phys. Rev. Lett.*, 95:247005, 2005.
- [30] T Sekihara, R Masutomi, and T Okamoto. *Phys. Rev. Lett.*, 111:057005, 2013.
- [31] P Wójcik. *J Supercond Nov Magn*, xx:xx, 2014.
- [32] P Wójcik and M Zegrodnik. *J. Phys. Condens. Matter*, 26:455302, 2014.
- [33] A A Shanenko, M D Croitoru, and F M Peeters. *Phys. Rev. B*, 78:024505, 2008.
- [34] D A Zocco, K Grube, F Eilers, T Wolf, and Löhneysen. *Phys. Rev. Lett.*, 111:057007, 2013.
- [35] T Terashima, K Kihou, M Tomita, S Tsuchiya, N Kikugawa, S Ishida, C H Lee, A Iyo, H Eisaki, and S Uji. *Phys. Rev. B*, 87:184513, 2013.
- [36] A Ptok and D Crivelli. *J. Low Temp. Phys.*, 172:226, 2013.
- [37] A Ptok. *Eur. Phys. J*, 87:2, 2014.
- [38] M Zegrodnik and J Spalek. *Phys. Rev. B*, 90:174597, 2014.
- [39] M Takahashi, T Mizushima, and K Machida. *PRB*, 89:064505, 2014.
- [40] T Mizushima, M Takahashi, and K Machida. *J. Phys. Soc. Jpn*, 83:023703, 2014.
- [41] P G de Gennes. *Superconductivity of Metals and Alloys*. Benjamin, New York, 1966.
- [42] I Kosztin, S Kos, M Stone, and A J Legget. *Phys. Rev. B*, 58:9365, 1998.
- [43] C M Wei and M Y Chou. *Phys. Rev. B*, 66:233408, 2002.
- [44] C M Wei and M Y Chou. *Phys. Rev. B*, 75:195417, 2007.
- [45] T Miller, M Y Chou, and T C Chiang. *Phys. Rev. Lett.*, 102:236803, 2009.